Defective Lung Vascular Development and Fatal Respiratory Distress in Endothelial NO Synthase–Deficient Mice

A Model of Alveolar Capillary Dysplasia?

Robin N.N. Han, Saeid Babaei, Malcolm Robb, Tony Lee, Ross Ridsdale, Cameron Ackerley, Martin Post, Duncan J. Stewart

Abstract—Endothelium-derived NO plays a critical role in the regulation of cardiovascular function and structure, as well as acting as a downstream mediator of the angiogenic response to numerous vascular growth factors. Although endothelial NO synthase (eNOS)–deficient mice are viable, minor congenital cardiac abnormalities have been reported and homozygous offspring exhibit high neonatal mortality out of proportion to the severity of these defects. The aim of the present report was to determine whether abnormalities of the pulmonary vascular development could contribute to high neonatal loss in eNOS-deficient animals. We now report that eNOS-deficient mice display major defects in lung morphogenesis, resulting in respiratory distress and death within the first hours of life in the majority of animals. Histological and molecular examination of preterm and newborn mutant lungs demonstrated marked thickening of saccular septae, with evidence of reduced surfactant material. Lungs of eNOS-deficient mice also exhibited a striking paucity of distal arteriolar branches and extensive regions of capillary hypoperfusion, together with misalignment of pulmonary veins, which represent the characteristic features of alveolar capillary dysplasia. We conclude that eNOS plays a previously unrecognized role in lung development, which may have relevance for clinical syndromes of neonatal respiratory distress. **(*Circ Res*. 2004;94:1115-1123.)**

Key Words: nitric oxide ■ angiogenesis ■ surfactant ■ respiratory distress syndrome ■ alveolar capillary dysplasia

NO is a multifaceted vasodilator that has also been shown to be an important regulator of vascular growth and remodeling.[1] NO has been implicated as a critical downstream mediator in the biological response to a variety of angiogenic growth factors,[2–5] mediating endothelial cell (EC) proliferation,[6] migration,[7] and vascular tube formation.[3] Adult eNOS-deficient mice ($eNOS^{-/-}$) exhibit marked defects in postnatal angiogenesis,[8] moderate systemic hypertension,[9] and mild elevation in pulmonary vascular resistance with an exaggerated pulmonary vasoconstrictor response to hypoxia.[10] Although $eNOS^{-/-}$ mice are viable, litter sizes are characteristically small, and these offspring exhibit minor abnormalities such as bicuspid aortic valve[11] and atrial septal defects.[12]

eNOS is strongly expressed in rodent[13] and ovine[14] fetal lungs at mid to late gestation, in both vascular endothelial as well as airway epithelial cells,[15] consistent with a possible role in the regulation of pulmonary vasculature and airway development. However, to date there has been no direct evidence implicating NO in fetal lung development, although recently eNOS has been shown to be involved in compensatory hyperplasia of postnatal lung[16] and in preventing loss of alveolarization during neonatal exposure to hypoxia.[17]

The paradox between the important role of NO in postnatal angiogenesis, yet the apparently normal embryonic vascular development in $eNOS^{-/-}$ animals could be explained by a high degree of redundancy, which often is associated with critical developmental steps. However, because the lung assumes its critical function as a gas exchange organ only after birth, even major abnormalities in lung development would not compromise embryonic and fetal survival, and would only be manifested postnatally. Indeed, Feng et al[12] have recently reported that although the number of pups initially born to $eNOS^{-/-}$ and WT mice was similar, eNOS-deficient offspring showed high rates of neonatal loss, out of proportion to the severity of congenital malformations. Therefore, we hypothesized that early postnatal mortality seen in the majority of $eNOS^{-/-}$ pups would be due to fatal neonatal respiratory distress caused by abnormalities in lung development.

Materials and Methods

$eNOS^{-/-}$ and wild-type (WT) C57BL/6J and BALBc mice were purchased from Jackson Laboratories (Bar Harbor, Maine) and bred according a protocol approved by the Animal Care Committee of St. Michael's Hospital. Immunostaining was performed using avidin-

Original received August 6, 2003; resubmission received December 5, 2003; revised resubmission received March 1, 2004; accepted March 2, 2004.

From Terrence Donnelly Heart Center (R.N.N.H., S.B., M.B., T.L., D.J.S.), Division of Cardiology, St Michael's Hospital and the Department of Medicine, University of Toronto; Hospital for Sick Children (R.R., C.A., M.P.), Toronto, Canada.

Correspondence to Dr Duncan J. Stewart, Director, Division of Cardiology and Dexter Man Chair, University of Toronto, Head of Cardiology, St Michael's Hospital, 30 Bond St, Suite 7081 Queen Wing, Toronto, Canada. E-mail Stewartd@smh.toronto.on.ca

Circulation Research **is available at http://www.circresaha.org** **DOI: 10.1161/01.RES.0000125624.85852.1E**

List of Genes of Interest and Primers for qRT-PCR

	Forward	Reverse
Ang-1	gagctccttgagaattacattgtgg	gagctccttgagaattacattgtgg
Tie-2	gacgatttacaaacagcgtctatcgg	gggagaatgtcactaagggtccag
Flk-1	ttaggtgcctccccataccctg	catttctggggtagtgtagtcagg
FGF-10	tttgactgtccgtacagtgtcctgg	aaattcctctattctctctttcagc
FGF-7	aaacgaggcaaagtgaaagggacc	ctttgaagttgcaatcctcattgcattc
FGF-R_2	aaacgggcctgatgggctgccctac	ataatctggggaagccgtgatctcc
TGF-β_2	tcagtggagttgtacgtattgtttcc	ggagtaacacacaataaataacccactg
TGF-β_1	gagctgcgcttgcagagattaaaatc	ttcagccactgccgtacaactcc
$VEGF^{164}$	catagagagaatgagcttcctacagc	tgctttctccgctctgaacaagg
eNOS	ttttgtcagttcagcacccagcgccc	tttggcggtgaggacttgtccaaac

biotin (ABC) immunoperoxidase method[18] as described in the expanded Materials and Methods section in the online data supplement available at http://circres.ahajournals.org. Ultrastructural analysis was performed in lungs from E20 and P0 (postpartum first hour) mice, fixed, and processed for transmission electron microscopy (TEM) as previously described,[19] using a JEM 1230 (JEOL USA, Inc) electron microscope.

Western Blot Analysis, Cell Proliferation, and Apoptosis Assays

Western blotting was performed on WT and $eNOS^{-/-}$ fetal lungs at E18, E20, and P0, as previously described.[20] Rat anti-mouse Ki67 (DAKO) [1:50] monoclonal antibody and immunoperoxidase method was used to detect proliferative cells in fetal and new born lung sections. TUNEL analyses were conducted using Apoptosis detection system [Fluorescein] (Promega), following manufacturer's instructions. Random images (10 per section) were captured and morphometric analyses [percentage of Ki67 (+) cells and TUNEL (+) cells] were conducted in a blinded fashion.

L-NAME Experiment

N^{ω}-nitro-L-arginine methyl ester (L-NAME) [nitric oxide synthase inhibitor] (Sigma) (90 mg/kg) was injected intraperitoneally in timed pregnant WT mice (C57BL/6J) and (BALBc) [n=3 from each genetic background] daily from E11 to E18 gestation. Control group (n=3) received equal volume of saline. Fetuses were harvested at E19.5 gestation for morphological analyses.

Fluorescent Microangiography

The chest cavity was opened and a 27½-gauge needle inserted into right ventricle. The fetal pulmonary arterial system was perfused with a solution of 1% low melting agarose (Sigma) containing a suspension of 0.2 μm fluorescent microspheres (1:10 [v/v]) (Molecular Probes) until free return of the agarose solution could be observed from a small incision in the left atrium. The fetuses were then fixed in 4% paraformaldehyde for 48 hours at 4°C and (150 μm) sections were cut on a vibratome [Leica *VT*1000S], counterstained with propidium iodide (Sigma) (5 μg/mL [wt/vol] in PBS) at room temperature for 10 minutes, washed in PBS, and mounted with mounting media. Images were captured by optical sectioning using confocal microscope (Bio-Rad "Radiance"). In separate experiments, WT and $eNOS^{-/-}$ fetuses at E20 gestation were given nitroglycerin (2 μg per fetus) intraperitoneally (IP), 10 minutes before performing fluorescent microangiography.

Quantitative RT-PCR

Total RNA was extracted from frozen fetal lung tissues as described in the online data supplement. The expression of genes of interest (Table) was analyzed by real-time PCR (ABI 7900HT, Applied Biosystems), using SYBR green PCR Core Reagents (ABI; see online data supplement for details). The results of real-time PCR were presented as absolute numbers (fg/reaction) measured against the standard curves. All measurements were performed in triplicates.

Lipid Mass Spectrophotometry for Newborn Lung Bronchoalveolar Lavage Fluid (BALFs)

Sterile PBS (50 μL) was infused into the trachea of newborn pups, and BALF samples (WT, n=5; $eNOS^{-/-}$, n=7) were extracted and flash frozen until further processing. At the time of analysis, the BALF samples were thawed on ice, centrifuged for 10 minutes, and extracted as previously described.[21] Lipid extracts were then directly infused at 15 μL/min into an API 4000 LC/MS/MS (MDS Sciex) using a Q1 scan from 100 to 1000 amu.

Statistical Analysis

All values were presented as mean±SEM. Statistical significance between groups was determined by one-way analysis of variance, followed by Bonferroni or unpaired *t* test, as appropriate. A value of $P<0.05$ was considered significant.

Results

Pregnant $eNOS^{-/-}$ and WT C57BL/6J mice were observed at term (8 litters for each) and during the immediate postpartum period (P0). Litter sizes of $eNOS^{-/-}$ animals varied from six to eight pups at birth, however some newborn $eNOS^{-/-}$ pups exhibited severe respiratory distress and were obviously cyanotic (Figure 1a). 40±5% of $eNOS^{-/-}$ offspring succumbed within the first hour of birth, whereas no neonatal mortality or respiratory distress was evident in pups of WT litters.

Defective Pulmonary Development in Mice

Lungs of WT mice showed normal saccular expansion and septal thinning at term (Figure 1b), whereas in $eNOS^{-/-}$ pups there was evidence of marked septal thickening and reduced airspaces (Figures 1d and 1f). Similarly, preterm (E20) $eNOS^{-/-}$ fetal lungs demonstrated abnormally compact lung structure compared with WT lungs (Figure 1c), often with only rudimentary saccules and indistinct bronchial structures (Figure 1e), although occasionally areas of reduced septation and abnormally large airspaces were observed (Figure 1g). Overall, the ratio of saccular to total parenchymal area in E20 $eNOS^{-/-}$ lungs was significantly reduced (0.020±0.01 and 0.11±0.03, $eNOS^{-/-}$ and WT, respectively; $P<0.05$, n=6 random fields from four animals per time points). There were no differences in cell proliferative index determined by Ki67-positive cells between WT and $eNOS^{-/-}$ at E20 (see online Figure S1 in the online data supplement). However, mutant animals demonstrated significantly less TUNEL-positive cells consistent with lower rate of apoptosis (see online Figure S1). Although fetal lungs from E16 $eNOS^{-/-}$ animals showed an apparently normal pseudoglandular histological pattern (Figure 2d) similar to WT E16 lungs (Figure 2c), there were scattered areas of parenchymal and interlobar hemorrhages (Figure 2d), suggestive of abnormal pulmonary vascular fragility, which was apparent even on gross inspection (Figure 2b). In contrast, there were no differences in either histological or gross appearance between WT and $eNOS^{-/-}$ embryonic lungs at earlier periods of gestation [E12/E13] (Figures 2e through 2h). In addition, $eNOS^{-/-}$ fetuses from embryonic day 18 to term demonstrated slight growth retardation when compared with WT mice (E20:

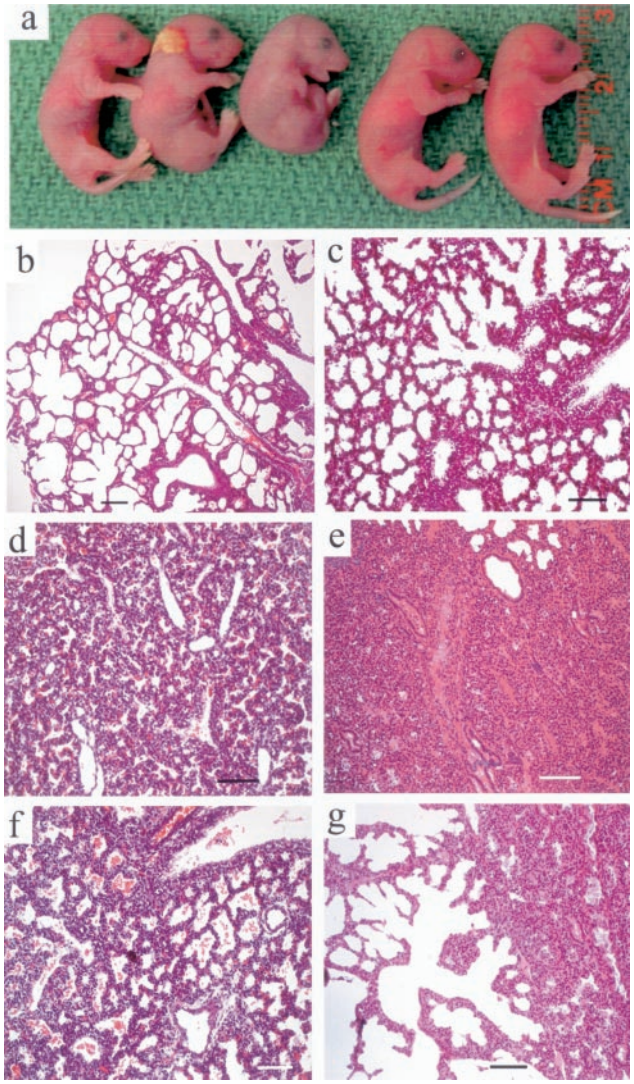

Figure 1. Abnormal lung morphology at term and immediately after birth in eNOS$^{-/-}$ mice. An eNOS$^{-/-}$ litter during the first hour of life (a): two neonates appeared normal (far right) while others showed varying levels of cyanosis and respiratory distress. Hematoxylin and eosin (H&E) staining lung sections from newborn (b, d, and f) and E20 fetal mice (c, e, and g). WT lungs showed normal saccular inflation and septal thinning at birth (b), whereas lungs from eNOS$^{-/-}$ neonates (d; still born) and (f; died of respiratory distress, 15 minutes after birth) exhibited reduced saccular volume and marked septal thickening. WT E20 fetal lung (c) showed well-developed saccular airway structure, whereas E20 eNOS$^{-/-}$ lungs displayed abnormally compact lungs with poorly developed saccules (e), although occasional regions of reduced septation and abnormally open lung architecture could be observed (g). Scale bars=50 μm.

982±22 and 1169±34 g, $P<0.001$); however, lung growth relative to body weight was not reduced. Newborn eNOS heterozygous mice did not show signs of respiratory distress at birth and the survival of litters was comparable to that of WT. Histological examination of eNOS$^{+/-}$ lungs demonstrated no lung abnormalities (data not shown). Interestingly, E19.5 lungs from WT fetuses of C57BL/6J or BALBc backgrounds exposed to L-NAME during mid to late gestation showed similar abnormalities to those of eNOS$^{-/-}$ animals (see online Figures S1e through S1h).

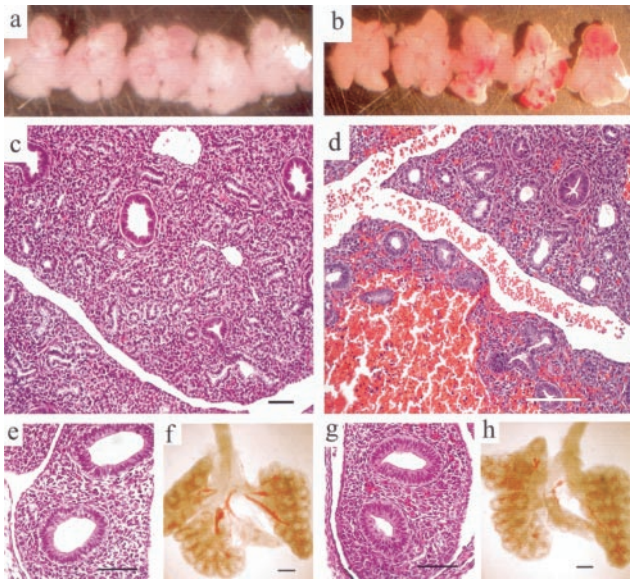

Figure 2. Embryonic (E12/E13) and fetal (E16) lung development. Fetal lungs at E16 from WT mice (a) had a normal gross appearance, whereas lungs from eNOS$^{-/-}$ mice (b) showed scattered subpleural hematomas. Both WT (c) and eNOS E16 fetal lung (d) exhibited normal pseudoglandular appearance on histological examination (H&E). However, lungs from eNOS$^{-/-}$ showed evidence of occasional parenchymal and interlobar hemorrhages. Embryonic lung development at mid gestation (e through h). E12 embryonic lung sections from WT (e) and eNOS$^{-/-}$ mice (g) demonstrated normal airway budding (H&E). Freshly isolated embryonic day E13 lungs from wild-type (WT) (f) and eNOS$^{-/-}$ mice (h) appeared normal on gross examination. Scale bars in c, d, e, and g=50 μm; f and h=100 μm.

Ultrastructural examination revealed well-developed basement membrane and matrix scaffolding in WT at E20 (Figure 3a). In contrast, lungs from E20 eNOS$^{-/-}$ demonstrated the absence of discernible basement membrane in the distal airways and vasculature with disorganization of extracellular matrix structure (Figure 3b). Capillaries of preterm WT lungs could be seen aligning with the saccular epithelium to form efficient air-blood barriers (Figures 3a and 3c), whereas those of eNOS$^{-/-}$ mice mostly remained deep within thickened septae (Figures 3b and 3d). The number of capillaries abutting saccular airspaces, quantified in 10 randomly chosen low-power fields (×2000), was significantly less in the eNOS$^{-/-}$ mice (1.3±1.4) compared with WT (4.0±2.2; $P<0.05$). In eNOS$^{-/-}$ lungs, grossly distended epithelial cells could be seen projecting into the saccular airspaces (Figures 3d and 3f) which, unlike the normal type II pneumocytes of WT lungs (Figure 3a), did not show evidence of lamellar bodies. Interestingly, preterm (Figure 3d) and newborn eNOS$^{-/-}$ lungs (data not shown) often displayed an absence of recognizable surfactant material within the airspaces, whereas abundant surfactant could be seen in the saccules of WT lungs at E20 (Figure 3c). Corresponding sections of lungs were stained with periodic acid-Schiff (PAS) and examined by light microscopy to assess the glycogen content of developing type II pneumocytes. In eNOS$^{-/-}$ mice, glycogen laden pneumocytes could be clearly seen protruding into the airspaces (Figure 3h). In contrast, lung sections from WT animals showed reduced PAS staining at term (Figure 3g), in

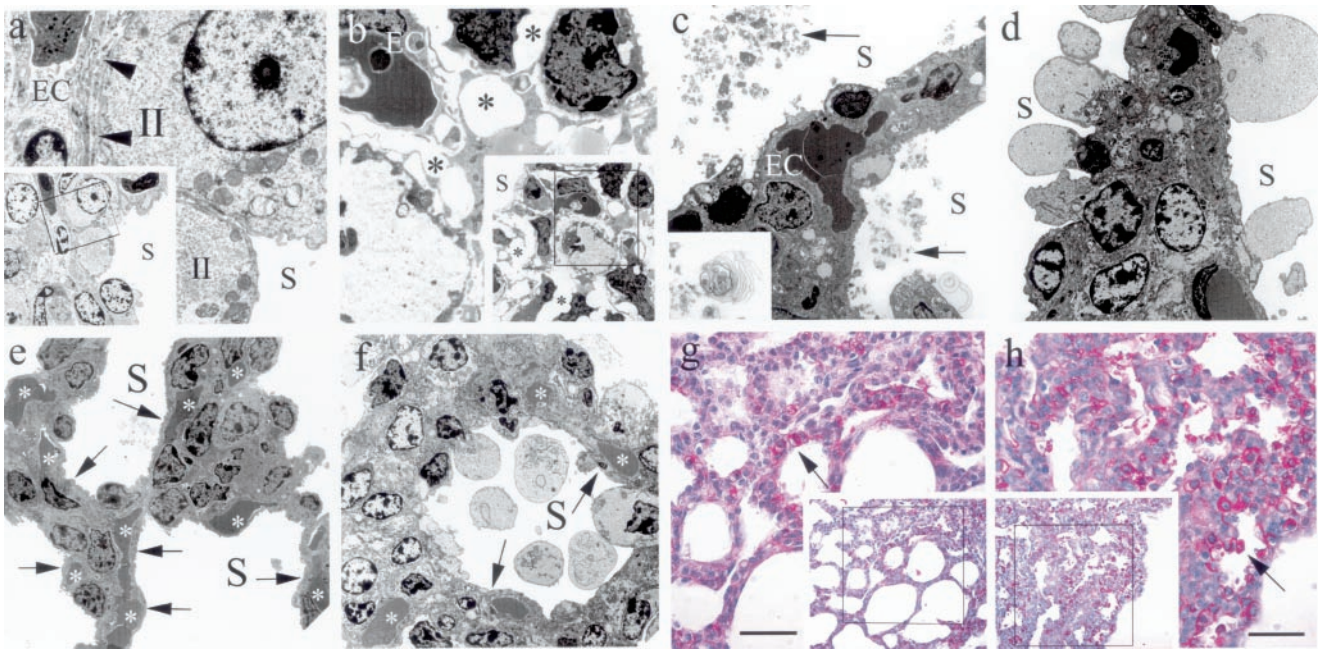

Figure 3. Transmission electron microscopy revealed normal pneumocyte maturation and matrix organization in WT lung at E20 (a) (inset, low-power image; box indicates enlarged region). Arrowheads point to mature basement membrane forming between and endothelial cell (EC) and a type II pneumocytes (II), identified by the presence of lamellar bodies. Ultrastructural examination of E20 eNOS$^{-/-}$ lung (b) revealed extracellular matrix disarray with large gaps (black asterisks) and the absence of any identifiable basement membrane between EC and pneumocyte-like cells (inset, low-power micrograph; box indicates enlarged region). Postnatal (PO) WT lung (c) showed normal septal thinning and pneumocyte maturation with surfactant material (arrows) clearly seen within saccular spaces (S) (inset, high-magnification image of a surfactant material). Electron micrography of an eNOS$^{-/-}$ E20 lung (d) showing distended cells protruding into the airspaces, lacking definite characteristics of mature pulmonary epithelial cells. Low-power image of WT-PO lung (e) with white asterisks indicating erythrocytes within abundant capillaries, whereas newborn eNOS$^{-/-}$ lung (f) exhibited a paucity of blood-air barriers (original magnifications: a and b, ×4000; c and d, ×2500; e and f, ×2000). Light micrographs of periodic acid-Schiff (PAS) showing a reduction in PAS (+) cells (arrows) in WT-PO lung (g) compared with eNOS$^{-/-}$ lung (h). g and h represent enlarged regions of boxes in insets (low magnification). Scale bars=50 μm.

keeping with the reduction in glycogen content seen in type II pneumocytes that are actively synthesizing and secreting surfactant. Based on similar PGP9.5 and CC10 immunostaining in WT and eNOS$^{-/-}$, no apparent defects in neuroepithelial cells and Clara cells were noted (data not shown).

Impaired Pulmonary Angiogenesis in eNOS$^{-/-}$ Mice

Cells expressing the endothelial marker, CD31 (PECAM-1), could be demonstrated by immunostaining in lung sections from both WT (Figure 4a) and newborn eNOS$^{-/-}$ mice P0 (Figures 4b and 4c). However the number of CD31-positive cells appeared to be reduced in both eNOS$^{-/-}$ as well as in E19.5 fetal lungs from WT mice exposed to L-NAME during mid to late gestation (Figure 4i). The 3-dimensional architecture of the distal pulmonary arterial tree was defined using fluorescent microangiography. WT lungs demonstrated uniform filling of the distal pulmonary arterial tree, with homogeneous perfusion of the microvasculature (Figure 4d). In contrast, lungs from eNOS$^{-/-}$ fetuses showed dramatic pruning of arteriolar branches and regions of marked capillary hypoperfusion (Figure 4e). Intraperitoneal nitroglycerin (NTG) administered to E20 fetuses 10 minutes before microangiography did not alter the angiographic appearance of eNOS$^{-/-}$ lungs (Figure 4k). Occasionally, eNOS$^{-/-}$ mice demonstrated evidence of misalignment of pulmonary veins, which were seen in anomalous locations adjacent to the lung pleura, running alongside arterial vessels and sharing a common adventitial sheath (Figures 4f and 4g). This, together with the lack of capillary in-growth into the alveolar septum, represents a characteristic feature of alveolar capillary dysplasia.[22] A similar histological appearance was evident in E19.5 lungs exposed to L-NAME (see online Figure S1h).

Growth Factor and eNOS Expression in WT and eNOS$^{-/-}$ Mice

The expression of eNOS and various angiogenic growth factors was examined using quantitative RT-PCR. WT animals showed a progressive increase in eNOS mRNA beginning at E14, and reaching statistical significance by E16 (Figure 5a), whereas no eNOS mRNA was detected in mutant animals (data not shown). In WT mice, there was a progressive increase from E16 to E20 in pulmonary mRNA levels for VEGF-A and angiopoietin-1 (Ang-1) and their receptors, flk-1 and Tie-2, respectively (Figures 5b through 5e). In contrast, the increase in expression of angiogenic factors was significantly reduced in eNOS$^{-/-}$ mice, whereas the housekeeping genes, β-actin (Figure 5f) and GADPH (data not shown), were constant and similar between WT and mutant mice.

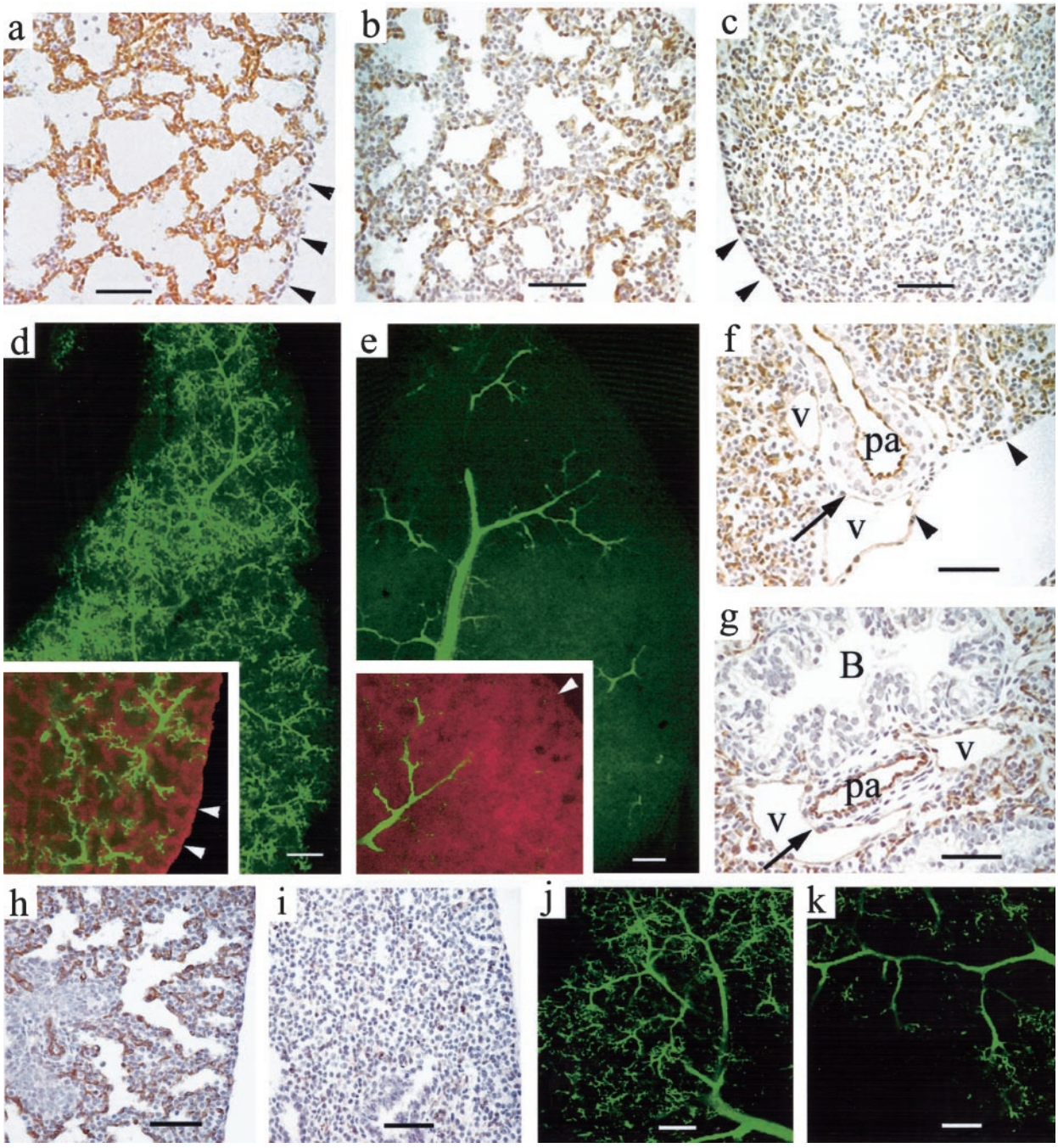

Figure 4. Abnormalities in pulmonary vascular development in eNOS-deficient or L-NAME–treated mice. CD31 immunostaining showing PECAM-1–positive cells in neonatal WT (a) and eNOS$^{-/-}$ (b and c). Fluorescent microangiography in E20 fetal lungs (d and e). WT mice displayed numerous small pulmonary arterioles (d, green fluorescence) extending into the capillary circulation (shown at higher magnification [inset] with propidium iodide nuclear counterstain in red fluorescence), whereas there were strikingly fewer arterioles in lungs from eNOS$^{-/-}$ (e) with regions of nearly complete discontinuity between the arterial and microvasculature circulations [higher magnification, inset]. Scale bars in d and e=100 μm. Angiographic appearance in WT (j) and eNOS$^{-/-}$ (k) fetal lung was not altered by pretreatment with nitroglycerin. Anomalous lung structure in eNOS-deficient mice (f and g). CD31-immunostained sections of lung from newborn eNOS$^{-/-}$ pups (f) revealed anomalous subpleural location of a small pulmonary artery [pa] and vein [v], and in some cases misalignment of pulmonary vessels (g), with veins sharing a common adventitia with a pulmonary artery (arrow; B, bronchiole). Arrowheads show pleural lining; scale bars=50 μm. CD31 (PECAM-1) immunostaining of E19.5 fetal lungs exposed to saline (h) or L-NAME (i) in utero.

Defective Surfactant in eNOS$^{-/-}$ Neonates

Expression of surfactant-associated proteins, SP-A, -B, and -C, markers for type II epithelial cell maturation, were not noticeably different between WT and eNOS$^{-/-}$ lungs (Figure 6d). In addition, immunohistochemistry of WT (Figure 6a) and eNOS$^{-/-}$ (Figures 6b and 6c) fetal lungs demonstrated similar pattern of SP-C expression. However, phosphatidylcholine (PC), the most abundant of the lipid components of surfactant[21] was dramatically reduced in bronchial alveolar lavage fluid from lungs of eNOS$^{-/-}$ at birth, compared with

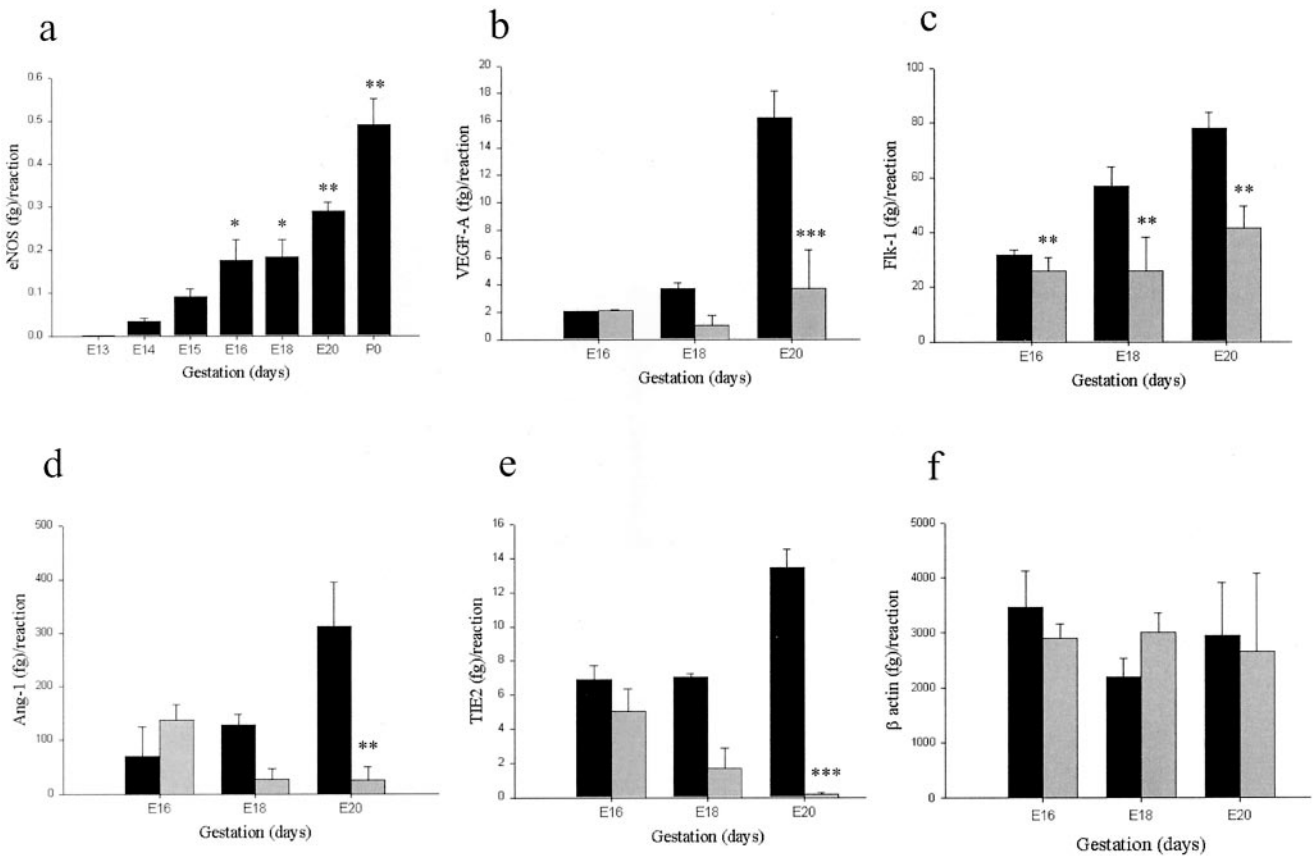

Figure 5. eNOS and angiogenic factor expression. WT lungs (black bars) showed a progressive increase in lung eNOS mRNA (a) by quantitative RT-PCR beginning at E14 and increasing to term (*$P<0.05$, **$P<0.01$ vs E13). Compared with WT mice, gene expression of VEGF-A (b), Flk-1 (c), Ang-1 (d), and TIE2 (e) was reduced in eNOS$^{-/-}$ (shaded bars) mice fetal lungs of E16-E20 mice, whereas β-actin (f) expression was comparable. *$P<0.05$, **$P<0.01$, and ***$P<0.001$.

that of WT pups (Figure 6e). Moreover, the surface active molecular species of surfactant, dipalmitoyl PC, was also significantly reduced in the lavage fluid (Figure 6f), suggesting that the surfactant produced by eNOS$^{-/-}$ mice lungs was both quantitatively and qualitatively defective.

Discussion

We report for the first time profound defects in lung morphogenesis in eNOS-deficient mice or mice treated with a NOS inhibitor, involving the pulmonary vascular tree and parenchyma. The pulmonary phenotype closely resembles the pathological features of alveolar capillary dysplasia (ACD), an increasingly recognized cause of persistent pulmonary hypertension of the newborn.[22,23]

The striking abnormalities in pulmonary vascular development in eNOS-deficient mice are consistent with the now well-accepted role of NO in angiogenesis in response to a variety of growth factors, most importantly VEGF.[2] There are two principle mechanisms by which VEGF contributes to blood vessel formation in the developing lung: vasculogenesis, which gives rise to the formation of capillaries from blood lakes; and angiogenesis, by which the more central vessels are generated,[24,25] including the arterial and arteriolar branches. Of note, abnormalities in the lung vasculature were not manifested in fetal eNOS-deficient mice until after E13, a time point at which the pulmonary expression of eNOS in WT fetal first began to increase (Figure 5a). The normal pattern of early vasculature development, together with the presence of capillary structures, albeit reduced in number, by immunostaining and electron microscopy in all lung sections examined, argues against a de novo failure of pulmonary vasculogenesis in this model. Rather, abnormalities were mainly related to the density of distal arteriolar branches, which develop mainly by angiogenesis.[24,25] The third process governing pulmonary development is the fusion between the central and peripheral systems, which is essential for establishing continuity between the arteriolar and capillary circulations.[25] The near complete lack of capillary perfusion in some regions of lungs from mutant animals raises the possibility that this critical fusion event was also disrupted in eNOS$^{-/-}$ mice. Intense vasospasm could be excluded as a mechanism because nitroglycerin pretreatment failed to improve pulmonary capillary perfusion in eNOS$^{-/-}$ lungs.

The apparent differential requirement for NO in pulmonary angiogenesis versus vasculogenesis in lung development is intriguing. Vasculogenesis and angiogenesis both appear to be under the control of VEGF.[26] The disruption of even a single copy of the VEGF gene results in embryonic lethality due to the failure of endothelial differentiation and blood vessels formation. To overcome this limitation, Galambos et al[27] engineered knock-in transgenic mice expressing only VEGF^{120}, which led to a selective impairment in the devel-

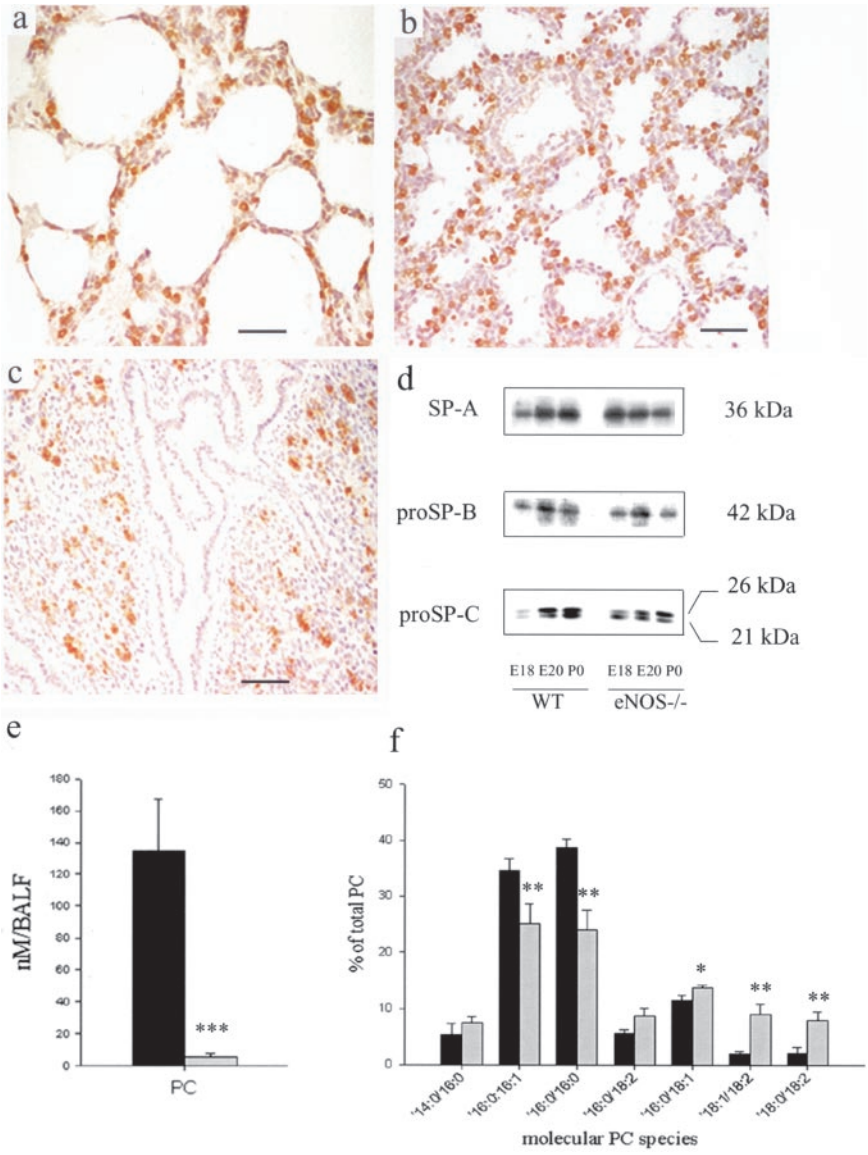

Figure 6. Surfactant-associated protein expression. Prosurfactant–associated protein C (SP-C) immunostaining could be seen in lung sections from WT (a) and eNOS$^{-/-}$ mice (b and c), at P0 (a and b) and E20 (c) (scale bars=50 μm). Western analyses (d) for SP-A, -B, and -C protein expression in WT and eNOS$^{-/-}$ (E18, E20, and P0) lungs. Phospholipid profile in bronchoalveolar lavage of newborn mice. Phosphatidylcholine (PC) content (e) in BALF was greatly reduced in eNOS$^{-/-}$ (shaded bars) P0 mice compared with WT mice (black bars). Comparison of PC molecular species (f) assessed by lipid mass spectrophotometry in BALF from WT (black bars) and eNOS$^{-/-}$ (shaded bars) P0 mice. *P<0.05, **P<0.01, and ***P<0.001 vs WT.

opment of the distal pulmonary arteriolar branches, strongly resembling the vascular defects of eNOS-deficient animals. However, the abnormalities in vascular development in VEGF$^{120/120}$ animals were less marked than described in the present report. Interestingly, the expression of a wide range of angiogenic growth factors was also markedly reduced in eNOS-deficient mice during late gestation, suggesting that NO may play a role not only in downstream signaling in angiogenesis, but also in regulation of angiogenic gene expression in the developing lung. Indeed, NO has been suggested to upregulate VEGF expression,[5] and recent studies from our group implicate eNOS in the regulation of Ang-1 expression as well.[28] Interestingly, occasional areas of parenchymal pulmonary hemorrhage were observed, especially at E16 gestation, possibly as a consequence reduced expression of vascular stabilizing factors such as Ang-1/TIE2 and TGF-β_1.[29] Therefore, it is possible that the defects in lung vascular development observed in eNOS$^{-/-}$ mice may have been in part secondary to a failure of a late gestational genetic program regulating the expression of angiogenic genes under the control of NO.

Lungs from mutant mice also exhibited reduced saccular area and thickening of the septae, again resembling features of the VEGF$^{120/120}$ transgenic model.[27] However, once more the abnormalities in the eNOS-deficient mice appeared more extensive. Not only did ultrastructural examination reveal a striking disarray of interstitial extracellular matrix and an absence of basement membrane in the distal airways and capillaries in eNOS$^{-/-}$ fetal lung, but also markedly swollen glycogen-laden epithelial cells could be seen protruding into the saccules. This finding is suggestive of a delay in maturation, because there is normally a reduction in glycogen content at term concurrent with increased surfactant secretion.[30] Interestingly, in lungs of eNOS$^{-/-}$ mice, there was no reduction in the expression of surfactant associated proteins (SP-A, -B, and -C) during late gestation which, taken together with the absence of lamellar bodies and the lack surfactant in lavage fluid, leads us to conclude that the defect may be at the level of the assembly of lipid-rich surfactant material, rather than protein synthesis.

Inadequate secretion of surfactant by pulmonary type II epithelial cells is a major cause of the respiratory distress

syndrome in neonates.[30] Recently, it has been recognized that angiogenic factors may play a role in the maturation of type II pneumocytes and the regulation of surfactant formation in the developing lung.[31] Animals deficient in hypoxia-inducible factor-2α (HIF-2α),[30] a key transcription factor regulating the levels of angiogenic gene expression, exhibited neonatal respiratory distress due to a selective defect in pneumocyte maturation and surfactant production. Although this phenotype also appears to be shared by eNOS$^{-/-}$-deficient mice, the latter again exhibited more severe and widespread abnormalities in pulmonary vascular and airway development. Because HIF-2α plays a pivotal role in the regulation of the expression of VEGF and other hypoxia-inducible angiogenic genes, this suggests that the abnormalities of pulmonary development in eNOS mutant mice cannot be ascribed solely to reduced angiogenic factor expression, but also reflect important and previously unrecognized direct effects of NO on endothelial and epithelial cell differentiation.

The marked abnormalities in epithelial differentiation and airway development in eNOS-deficient mice raise important questions about cross-talk between endothelial and epithelial cells in the developing lung. Previous studies have shown that inhibition of angiogenesis induced by VEGF receptor blockade had an important effect of lung development in neonatal mice,[32] consistent with the view that the differentiation and maturation of airways may be under the control of the vascular signals. However, it is important to note that eNOS expression is not confined to the vascular endothelium, and it is also present in the epithelium of developing airways.[14] Also, NO has been shown to modulate epithelial cell migration,[33] functioning to regulate the cycling of integrin-matrix binding at the leading edge of migrating cells. Therefore in the present model, it is not possible to dissociate the paracrine effects of endothelial-derived NO on epithelial cell maturation from possible autocrine actions. Further experiments using targeted knock-out or knock-in strategies to selectively alter endothelial and epithelial eNOS expression will likely provide valuable insight into this important question.

The pulmonary vascular phenotype of eNOS$^{-/-}$ mice shares surprising similarities with a new clinical syndrome, alveolar capillary dysplasia (ACD), described in infants with persistent pulmonary hypertension of the newborn refractory to vasodilator treatment.[22] This is a uniformly fatal disorder that is characterized by a deficiency of alveolar capillary in-growth and failure to form normal air-blood barriers by close apposition between endothelial and type I epithelial cells. In eNOS-deficient animals, the formation of the air-blood barrier may have been impeded by the failure of development of both endothelial and epithelial basement membranes, which normally fuse to form the capillary-alveolar membrane. Infants with ACD often display misalignment of pulmonary veins, with both venous and arterial vessels sharing a common adventitial sheath,[22] an anomaly that was also found in the eNOS$^{-/-}$ lungs (Figures 4f and 4g). ACD is also associated with other congenital defects, including phocomelia, bicuspid aortic valve, and atrial septal defects,[22] which interestingly have all been reported in eNOS$^{-/-}$ mice.[11,12,34] As well, heterogenous areas of abnormally open airspaces lungs were occasionally noted in eNOS$^{-/-}$ lungs at late gestation, reminiscent of the histological features of bronchopulmonary dysplasia (BPD), which occurs as a complication in premature neonates subjected to ventilatory support for severe hypoxemia.[35] Reduced expression of PECAM-1 (CD31), Flt-1, and Tie2 has been reported in lungs of infants dying of BPD,[36] providing further evidence linking this condition to disordered angiogenesis. Given the recently described impairment of alveolarization in eNOS$^{-/-}$ exposed to hypoxia,[17] it is possible that abnormal NO production might contribute to abnormal alveolar vascularization and loss of septation in this condition.

Abnormal pulmonary morphogenesis and maturation represents a significant problem in the immediate neonatal period, which together with prematurity-related lung diseases results in substantial morbidity and mortality due to respiratory distress and neonatal pulmonary hypertension. The present report provides novel evidence of a previously unrecognized contribution of NO to lung vascular and airway development and maturation. Thus, pharmacological or genetic manipulation of NO production in the perinatal period may represent a therapeutic strategy for the treatment or prevention of respiratory distress in clinical conditions associated with abnormalities in lung morphogenesis or premature delivery.

Acknowledgments

This work was supported by the Canadian Institutes of Health Research grant No. MPO-57726.

References

1. Moncada S, Palmer RM, Higgs EA. Nitric oxide: physiology, pathophysiology, and pharmacology. *Pharmacol Rev*. 1991;43:109–142.
2. Ziche M, Morbidelli L, Choudhuri R, Zhang HT, Donnini S, Granger HJ, Bicknell R. Nitric oxide synthase lies downstream from vascular endothelial growth factor-induced but not basic fibroblast growth factor-induced angiogenesis. *J Clin Invest*. 1997;99:2625–2634.
3. Babaei S, Teichert-Kuliszewska K, Monge JC, Mohamed F, Bendeck MP, Stewart DJ. Role of nitric oxide in the angiogenic response in vitro to basic fibroblast growth factor. *Circ Res*. 1998;82:1007–1015.
4. Inoue N, Venema RC, Sayegh HS, Ohara Y, Murphy TJ, Harrison DG. Molecular regulation of the bovine endothelial cell nitric oxide synthase by transforming growth factor-β1. *Arterioscler Thromb Vasc Biol*. 1995; 15:1255–1261.
5. Dulak J, Jozkowicz A, Dembinska-Kiec A, Guevara I, Zdzienicka A, Zmudzinska-Grochot D, Florek I, Wojtowicz A, Szuba A, Cooke JP. Nitric oxide induces the synthesis of vascular endothelial growth factor by rat vascular smooth muscle cells. *Arterioscler Thromb Vasc Biol*. 2000;20:659–666.
6. Ziche M, Morbidelli L, Masini E, Granger H, Geppetti P, Ledda F. Nitric oxide promotes DNA synthesis and cyclic GMP formation in endothelial cells from postcapillary venules. *Biochem Biophys Res Commun*. 1993; 192:1198–1203.
7. Babaei S, Stewart DJ. Overexpression of endothelial NO synthase induces angiogenesis in a co-culture model. *Cardiovasc Res*. 2002;55: 190–200.
8. Murohara T, Asahara T, Silver M, Bauters C, Masuda H, Kalka C, Kearney M, Chen D, Symes JF, Fishman MC, Huang PL, Isner JM. Nitric oxide synthase modulates angiogenesis in response to tissue ischemia. *J Clin Invest*. 1998;101:2567–2578.
9. Huang PL, Huang Z, Mashimo H, Bloch KD, Moskowitz MA, Bevan JA, Fishman MC. Hypertension in mice lacking the gene for endothelial nitric oxide synthase. *Nature*. 1995;377:239–242.
10. Fagan KA, Morrissey B, Fouty BW, Sato K, Harral JW, Morris KG Jr, Hoedt-Miller M, Vidmar S, McMurtry IF, Rodman DM. Upregulation of nitric oxide synthase in mice with severe hypoxia-induced pulmonary hypertension. *Respir Res*. 2001;2:306–313.

11. Lee TC, Zhao YD, Courtman DW, Stewart DJ. Abnormal aortic valve development in mice lacking endothelial nitric oxide synthase. *Circulation*. 2000;101:2345–2348.
12. Feng Q, Song W, Lu X, Hamilton JA, Lei M, Peng T, Yee SP. Development of heart failure and congenital septal defects in mice lacking endothelial nitric oxide synthase. *Circulation*. 2002;106:873–879.
13. North AJ, Star RA, Brannon TS, Ujiie K, Wells LB, Lowenstein CJ, Snyder SH, Shaul PW. Nitric oxide synthase type I and type III gene expression are developmentally regulated in rat lung. *Am J Physiol*. 1994;266:L635–L641.
14. Sherman TS, Chen Z, Yuhanna IS, Lau KS, Margraf LR, Shaul PW. Nitric oxide synthase isoform expression in the developing lung epithelium. *Am J Physiol*. 1999;276:L383–L390.
15. Shaul PW, North AJ, Wu LC, Wells LB, Brannon TS, Lau KS, Michel T, Margraf LR, Star RA. Endothelial nitric oxide synthase is expressed in cultured human bronchiolar epithelium. *J Clin Invest*. 1994;94: 2231–2236.
16. Leuwerke SM, Kaza AK, Tribble CG, Kron IL, Laubach VE. Inhibition of compensatory lung growth in endothelial nitric oxide synthase-deficient mice. *Am J Physiol Lung Cell Mol Physiol*. 2002;282: L1272–L1278.
17. Balasubramaniam V, Tang JR, Maxey A, Plopper CG, Abman SH. Mild hypoxia impairs alveolarization in the endothelial nitric oxide synthase-deficient mouse. *Am J Physiol Lung Cell Mol Physiol*. 2003;284: L964–L971.
18. Hsu SM, Raine L, Fanger H. Use of avidin-biotin-peroxidase complex (ABC) in immunoperoxidase techniques: a comparison between ABC and unlabeled antibody (PAP) procedures. *J Histochem Cytochem*. 1981;29: 577–580.
19. Kent G, Iles R, Bear CE, Huan LJ, Griesenbach U, McKerlie C, Frndova H, Ackerley C, Gosselin D, Radzioch D, O'Brodovich H, Tsui LC, Buchwald M, Tanswell AK. Lung disease in mice with cystic fibrosis. *J Clin Invest*. 1997;100:3060–3069.
20. Han RN, Post M, Tanswell AK, Lye SJ. Insulin-like growth factor-I receptor-mediated vasculogenesis/angiogenesis in human lung development. *Am J Respir Cell Mol Biol*. 2003;28:159–169.
21. Postle AD, Heeley EL, Wilton DC. A comparison of the molecular species compositions of mammalian lung surfactant phospholipids. *Comp Biochem Physiol A Mol Integr Physiol*. 2001;129:65–73.
22. Rabah R, Poulik JM. Congenital alveolar capillary dysplasia with misalignment of pulmonary veins associated with hypoplastic left heart syndrome. *Pediatr Dev Pathol*. 2001;4:167–174.
23. Cassidy J, Smith J, Goldman A, Haynes S, Smith E, Wright C, Haworth S, Davis P, Firmin R, Kasem K, Davis C. The incidence and characteristics of neonatal irreversible lung dysplasia. *J Pediatr*. 2002;141: 426–428.
24. deMello DE, Sawyer D, Galvin N, Reid LM. Early fetal development of lung vasculature. *Am J Respir Cell Mol Biol*. 1997;16:568–581.
25. Stenmark KR, Gebb SA. Lung vascular development: breathing new life into an old problem. *Am J Respir Cell Mol Biol*. 2003;28:133–137.
26. Ferrara N, Carver-Moore K, Chen H, Dowd M, Lu L, O'Shea KS, Powell-Braxton L, Hillan KJ, Moore MW. Heterozygous embryonic lethality induced by targeted inactivation of the VEGF gene. *Nature*. 1996;380:439–442.
27. Galambos C, Ng YS, Ali A, Noguchi A, Lovejoy S, D'Amore PA, deMello DE. Defective pulmonary development in the absence of heparin-binding vascular endothelial growth factor isoforms. *Am J Respir Cell Mol Biol*. 2002;27:194–203.
28. Babaei S, Teichert-Kuliszewska K, Zhang Q, Jones N, Dumont DJ, Stewart DJ. Angiogenic actions of angiopoietin-1 require endothelium-derived nitric oxide. *Am J Pathol*. 2003;162:1927–1936.
29. Carmeliet P. Mechanisms of angiogenesis and arteriogenesis. *Nat Med*. 2000;6:389–395.
30. Compernolle V, Brusselmans K, Acker T, Hoet P, Tjwa M, Beck H, Plaisance S, Dor Y, Keshet E, Lupu F, Nemery B, Dewerchin M, Van Veldhoven P, Plate K, Moons L, Collen D, Carmeliet P. Loss of HIF-2α and inhibition of VEGF impair fetal lung maturation, whereas treatment with VEGF prevents fatal respiratory distress in premature mice. *Nat Med*. 2002;8:702–710.
31. Abman SH. Bronchopulmonary dysplasia: "a vascular hypothesis." *Am J Respir Crit Care Med*. 2001;164:1755–1756.
32. Le Cras TD, Markham NE, Tuder RM, Voelkel NF, Abman SH. Treatment of newborn rats with a VEGF receptor inhibitor causes pulmonary hypertension and abnormal lung structure. *Am J Physiol Lung Cell Mol Physiol*. 2002;283:L555–L562.
33. Noiri E, Peresleni T, Srivastava N, Weber P, Bahou WF, Peunova N, Goligorsky MS. Nitric oxide is necessary for a switch from stationary to locomoting phenotype in epithelial cells. *Am J Physiol*. 1996;270: C794–C802.
34. Gregg AR, Schauer A, Shi O, Liu Z, Lee CG, O'Brien WE. Limb reduction defects in endothelial nitric oxide synthase-deficient mice. *Am J Physiol*. 1998;275:H2319–H2324.
35. Coalson JJ. Pathology of new bronchopulmonary dysplasia. *Semin Neonatol*. 2003;8:73–81.
36. Bhatt AJ, Pryhuber GS, Huyck H, Watkins RH, Metlay LA, Maniscalco WM. Disrupted pulmonary vasculature and decreased vascular endothelial growth factor, Flt-1, and TIE-2 in human infants dying with bronchopulmonary dysplasia. *Am J Respir Crit Care Med*. 2001;164: 1971–1980.